Journal of Organometallic Chemistry, 342 (1988) 353–371
Elsevier Sequoia S.A., Lausanne – Printed in The Netherlands

Nature of the hydrogen bridge in transition metal complexes

III *. Characteristics of the metal–hydrogen–metal bridge bond in binuclear transition metal complexes with mixed bridges of the type $[L_3M\overset{H}{\underset{L}{<L>}}ML_3]^n$ on the basis of molecular orbital calculations

Bogusława Jeżowska-Trzebiatowska and Barbara Nissen-Sobocińska

Institute for Low Temperature and Structure Research, Polish Academy of Sciences, Plac Katedralny 1, 50–950 Wrocław (Poland)

(Received September 15th, 1987)

Abstract

For the comparison of the roles played by the hydrogen atom and other ligands such as chlorine atoms and carbonyl groups in formation of triple mixed bridges in the

$[L_3M\overset{H}{\underset{L}{<L>}}ML_3]^{3-}$

complexes, electronic structure calculations were carried out by use of the parameter-free Fenske-Hall method for the complexes

$(CO)_3Fe\overset{CO}{\underset{CO}{<CO>}}Fe(CO)_3$, $[(CO)_3Fe\overset{H}{\underset{CO}{<CO>}}Fe(CO)_3]^-$ and $[Cl_3Mo\overset{H}{\underset{Cl}{<Cl>}}MoCl_3]^{3-}$.

The influence of the bridge ligands on the terminal ligands was described i.e. the *trans* effect of the bridging H, Cl and CO ligands was compared.

Introduction

Transition metal complexes, which contain mixed bridges, viz. (M–H–M) bridges supported by one or more other analogous bridges constitute a large group. These bridging ligands may be phosphines, chlorides, hydroxylic and carbonyl groups [1].

* For part II see Ref. 11

0022-328X/88/$03.50

In previous papers we have discussed the electronic structure of carbonyl binuclear complexes containing only single or double hydrogen bridges [2].

Herein we describe two geometrically similar complexes, the iron complex

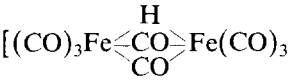

and the molybdenum complex

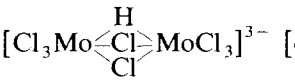

There are interesting differences in the various structural parameters on going from the "parent" complexes with triple chloride or carbonyl bridges to mixed bridge complexes containing at least one hydrogen bridge. For

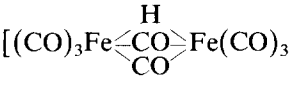

the Fe–Fe distance of 2.521 A [3] is almost the same as that for

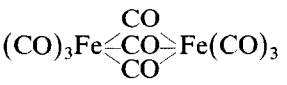

(2.524 Å) [5]. Another feature is that the average Fe–C distances for the terminal carbonyls in the positions *cis* ($Fe-C_T^c$) and *trans* ($Fe-C_T^t$) to the bridging hydrogen atom are the same. This indicates that the *trans* effect of both the bridging hydrogen atom and bridging carbonyl groups is the same.

The Mo–Mo distance depends to some extent on the type of cation to which the

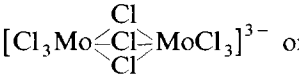

anion is linked in the crystal lattice [4,6].

However, only the difference in the Mo–Mo distance on going from

is significant, and was found to be shorter by about 0.2 Å. The bonds between the molybdenum atoms and terminal chlorine atoms in positions *trans* to the bridging hydrogen atom ($Mo-Cl_T^t$) are elongated with respect to those between the molybdenum atoms and the terminal chlorine atoms in positions *cis* to the bridging hydrogen atom ($Mo-Cl_T^c$).

We emphasize that on changing to the hydrogen-bridged complex the length of bonds between the molybdenum atoms and bridging chlorine atoms ($Mo-Cl_B$) remains almost unchanged. Also the $Mo-Cl_T^c$ bond lengths are almost equal to those between the metal atoms and terminal ligands ($Mo-Cl_T$) in the

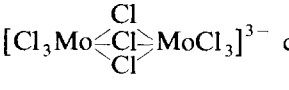

complex.

All of this indicates that the *trans* effect of the bridging hydrogen atom is stronger than that of the bridging chlorine atoms. In this paper we present the

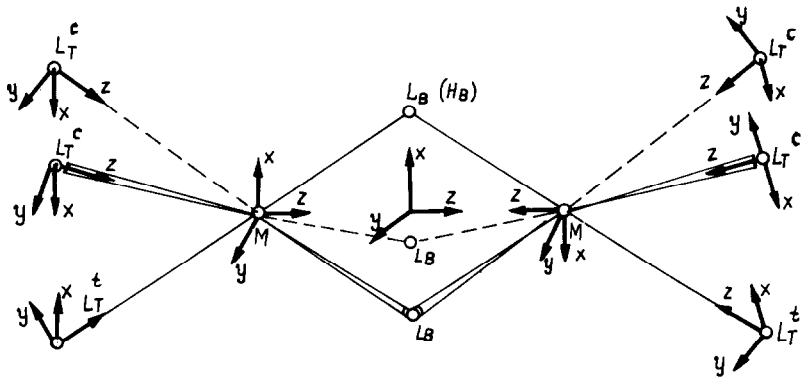

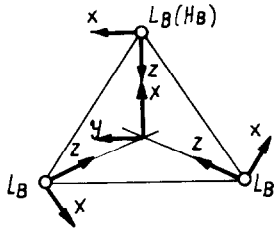

Fig. 1. Coordinate systems assumed in the calculations for the complexes $[L_3M\langle\begin{smallmatrix}L\\L\end{smallmatrix}\rangle ML_3]^n$ and $[L_3M\langle\begin{smallmatrix}H\\L\end{smallmatrix}\rangle ML_3]^m$.

results of molecular orbital calculations by use of the parameter-free Fenske–Hall method [7] for the dimeric iron carbonyls

$$(CO)_3Fe\langle\begin{smallmatrix}CO\\CO\\CO\end{smallmatrix}\rangle Fe(CO)_3 \text{ and } [(CO)_3Fe\langle\begin{smallmatrix}H\\CO\\CO\end{smallmatrix}\rangle Fe(CO)_3]^-.$$

The structural parameters for calculations were assumed in accordance with the respective X-ray diffraction studies [3,5].

The electronic structure of

$$[Cl_3Mo\langle\begin{smallmatrix}Cl\\Cl\\Cl\end{smallmatrix}\rangle MoCl_3]^{3-}$$

was calculated previously by Ginsberg, who used the X_α-SCF method [8], and by Natkaniec [9] who used the Fenske-Hall method, but the electronic structure of

$$[Cl_3Mo\langle\begin{smallmatrix}H\\Cl\\Cl\end{smallmatrix}\rangle MoCl_3]^{3-}$$

Table 1

Bond lengths (Å) used in the calculations

Complex	M–M	$M-H_B$	$M-L_B$	$M-L_T$	Ref.
$(CO)_3Fe\langle^{CO}_{CO}\rangle Fe(CO)_3$	2.521	–	1.99	1.79	3
$[(CO)_3Fe\langle^{H}_{CO}\rangle Fe(CO)_3]^-$	2.521	1.61	1.99	1.79	3
$[Cl_3Mo\langle^{H}_{Cl}\rangle MoCl_3]^{3-}$	2.371	1.68	2.477	2.477	4

was calculated by use of the X_α-SCF method by Cotton et al. [10].

In order to compare the electronic structures of the bridges cores

$Mo\langle^{Cl}_{Cl}\rangle Mo$ and $Mo\langle^{H}_{Cl}\rangle Mo$

we carried out the calculations by use of the Fenske–Hall method for

$[Cl_3Mo\langle^{H}_{Cl}\rangle MoCl_3]^{3-}$,

we also refer to the results of calculations for

$[Cl_3Mo\langle^{Cl}_{Cl}\rangle MoCl_3]^{3-}$,

which were taken from ref. 9.

For our calculations we used the X-ray structural data for

$[Cl_3Mo\langle^{H}_{Cl}\rangle MoCl_3]^{3-}$

on the assumption that bond lengths for $Mo-Cl_T^c$ and $Mo-Cl_T^t$ are the same [4]. Figure 1 depicts the coordinate systems on atoms assumed for the calculations and Table 1 lists the bond lengths.

Results and discussion

1. Comparison of the Fe–H–Fe and Fe–CO–Fe bridge bonds in the $(CO)_3Fe\langle^{CO}_{CO}\rangle Fe(CO)_3$ *and* $[(CO)_3Fe\langle^{H}_{CO}\rangle Fe(CO)_3]^-$ *complexes*

The filled energy levels determined by use of the Fenske–Hall method in the valence orbital base for

$(CO)_3Fe\langle^{CO}_{CO}\rangle Fe(CO)_3$

can be classed, according to increasing energy, as follows:

(*1*) from −44.85 to −32.80 eV, levels which correspond to σ-MOs of terminal groups (CO_T)

(*2*) from −24.95 to −22.45 eV levels which correspond to Π^bMOs of CO_T groups
(*3*) −22.25 eV energy level ($5a_1$) mainly of the σ-MO character of the bridging carbonyl groups (CO_B)
(*4*) the −21.27 and −21.23 eV energy levels ($4a_2''$ and $6a_1'$ respectively), mainly of the δ-MO character of the CO_T groups and with a slight contribution by the Fe 4*s* (2%) and Fe4*p*(6%) AOs
(*5*) −20.86 eV energy level ($5e_1$) mainly of the σ-MO character of the CO_B groups (about 80%), i.e. which partly corresponds to the Fe–CO–Fe bridge bonds
(*6*) from −19.96 to −18.81 eV levels of the Π^bMO character of the CO_T groups
(*7*) from −18.67 to −17.72 eV levels of the the σ and Π^b type MOs of CO_B groups
(*8*) the −16.25 eV energy level ($8e'$) of the σ(44%) an Π^b type MOs of the CO_B groups and the $3d_{xz}$ and $3d_{yz}$ AOs (24%) of the Fe atoms, those that correspond to the Fe–CO–Fe bridge bonds
(*9*) the −15.28 and −14.89eV energy levels ($6e''$ and $9e'$ respectively), of the Π^bMO character of the (CO_T) groups (ca. 50%), and the $3d_{xz}$,$3d_{yz}$ and $4p_x$,$4p_y$ AO character of the Fe atoms (ca. 20%) of those that correspond to the Fe–CO_T bonds
(*10*) from −11.34 to −10.85 eV, levels of the Π^a MO character of CO_T and CO_B groups (about 30%) and of the $3d_{z^2}$, $3d_{x^2-y^2}$, $3d_{xy}$, 4*s* AOs of the Fe atoms (from 50 to 70%), those that correspond to the 3*d* Fe→Π-ci^aCO_T or 3*d* Fe→$\Pi^a CO_B$ bonding interactions
(*11*) −8.86 eV energy level of the Π^a MO ($8e'$) character of the CO_B and CO_T groups and $3d_{xz}$,$3d_{yz}$,$4p_x$, $4p_y$ AOs of the Fe atoms (about 70%), which also correspond to the 3*d*Fe→$\Pi^a CO_B$ or 3*d*Fe→$\Pi^a CO_T$ bonding interactions.

The lowest unfilled molecular level $10a_1$ (LUMO) corresponds to the $3d_{z^2}$Fe→$\Pi^a CO_T$ interaction.

The group of last filled molecular levels with fairly high participation of the metal AOs, viz. $6a_2''$, $9a_1''$, $10e'$ and $7e''$ does not contribute to the direct metal–metal bond. This is because the metal AOs provide equal contributions to the molecular orbitals of bonding and antibonding character with respect to the M–M bond (Table 2, Fig. 2).

Yet, since the $8e''$ (HOMO) is antibonding with respect to direct M–M interaction, the

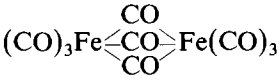

complex shows antibonding Fe–Fe interaction, a feature which is also reflected in the fairly high negative Fe–Fe overlap population of −0.166 (Table 4). Thus, the molecular level scheme proposed as a result of our calculations by use of the Fenske–Hall method for this complex is quantitatively and qualitatively consistent with that proposed previously, in which the SCF-HF method by Heiser et al. was used.

Changes take place in the electronic structure of

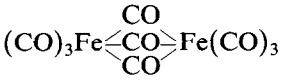

when one CO_B group is replaced with a hydrogen atom at the same position, only in

Table 2

Energies and compositions of the highest occupied molecular levels of $(CO)_3Fe\langle^{CO}_{CO}\rangle Fe(CO)_3$ with D_{3h} symmetry

MO	Energy (eV)	Largest contributions by valence atomic orbitals (%)					
$10a_1'$ LUMO	−5.63	p_y(O)	38	p_y(C)	31	$3d_{z^2}$(Fe)	25
$8e''$ HOMO	−8.86	$\underline{3d_{xz}}$(Fe) [a] $\overline{3d_{yz}}$	41	$\underline{p_x(Fe)}$ [a] p_y	18	$p_y(O_B)$	18
$7e''$	−10.85	$\underline{3d_{xz}}$(Fe) [a] $\overline{3d_{yz}}$	72	$p_y(O_B)$	13	p_y(O)	6
$10e'$	−10.87	$\underline{3d_{xy}}$(Fe)[a] $\overline{3d_{x^2-y^2}}$	72	$p_x(O_B)$	9	$\underline{3d_{xz}}$(Fe) [a] $\overline{3d_{yz}}$	5
$9a_1'$	−11.23	$3d_{z^2}$(Fe)	67	p_y(O)	20	s(Fe)	7
$6a_2''$	−11.34	$3d_{z^2}$(Fe)	31	$p_y(O_B)$	27	s(Fe)	18
$9e'$	−14.89	p_x(O)	27	p_y(O)	21	$\underline{p_x}$(Fe) [a] p_y	17
$6e''$	−15.28	p_y(O)	28	p_x(O)	26	$\underline{3d_{xz}}$(Fe) [a] $\overline{3d_{yz}}$	21
$8e'$	−16.25	$p_z(O_B)$	29	$\underline{3d_{xz}}$(Fe) [a] $\overline{3d_{yz}}$	24	$p_z(C_B)$	15
$8a_1'$	−17.72	$p_x(O_B)$	70	$p_x(C_B)$	30		
$7a_1'$	−17.73	$p_z(O_B)$	58	$p_z(C_B)$	20	$s(O_B)$	8
$7e'$	−18.31	$p_x(O_B)$	53	$p_x(C_B)$	37	$p_z(O_B)$	6
$5e''$	−18.35	$p_y(O_B)$	54	$p_y(C_B)$	37	$\underline{3d_{xz}}$(Fe) [a] $\overline{3d_{yz}}$	3
$5a_2''$	−18.67	$p_y(O_B)$	49	$p_y(C_B)$	42	s(Fe)	4
$1a_1''$	−18.81	p_x(O)	87	p_x(C)	13		
$1a_2'$	−18.81	p_x(O)	87	p_x(C)	13		

[a] Doubly degenerated molecular level.

those levels which have mainly MO character of CO_B groups or correspond to the Fe–CO–Fe bridge bonds as shown in Fig. 3. Thus, the three non-bonding levels: $5a_2'$, $7a_1'$ and $8a_1'$ which have exclusively σ or Π^b MO character of the CO_B groups in

$(CO)_3Fe\langle^{CO}_{CO}\rangle Fe(CO)_3$

were replaced with the $13a_1'$ level having the MOs σ character of the CO_B groups (70%) and 1s AO of hydrogen atom (7%), within the same energy range (Tables 2, 3).

The $13a_1$ level also includes 9% of the $4p_z$ AOs of the metal atoms, so it may be considered as corresponding simultaneously to the Fe–H–Fe and Fe–CO–Fe bridge bonds.

The higher $8e'$ level of the Fe–CO–Fe bridge bond character in the dimer with a triple carbonyl bridge was split into two levels: $9b_2$ and $14a_1$. The $9b_2$ level retains the Fe–CO–Fe bond character whereas the $14a_1$ level takes on Fe–H–Fe bridge bond character. Thus the H1s AO simply exchanges with the molecular orbitals of the bridging CO group in the formation of the bridge levels. Moreover, the $9e'$ level

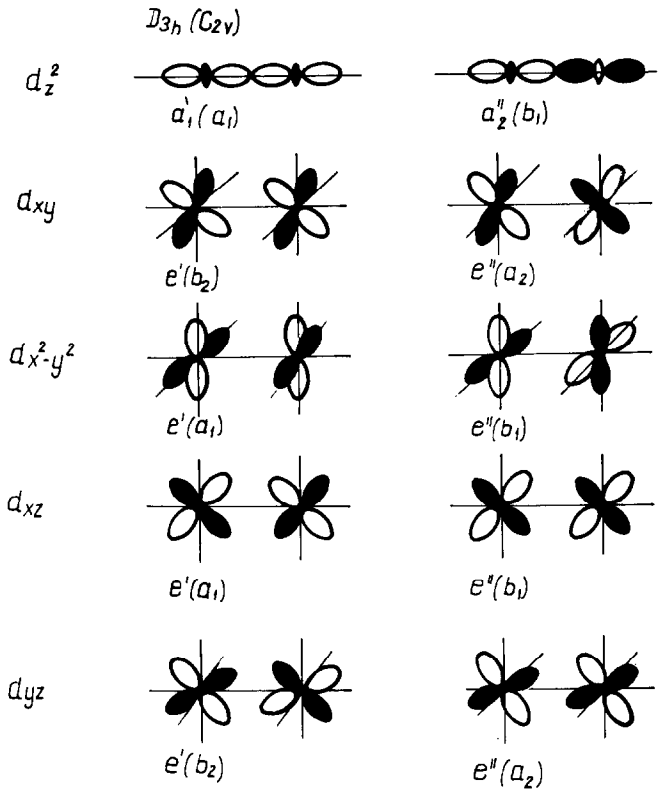

Fig. 2. Symmetry adapted linear combinations of the d atomic orbitals of the metal atoms.

which corresponds exclusively to the Fe–CO_T bonds in

$(CO)_3Fe\langle^{CO}_{CO}\rangle Fe(CO)_3$, in $[(CO)_3Fe\langle^{H}_{CO}\rangle Fe(CO)_3]^-$

splits into $10b_2$ and $15a_1$ levels.

The $10b_2$ level keeps the same character as the $9e'$ level whereas the $15a_1$ level corresponds to the Fe–H–Fe bridge bond because of a fairly large contribution by the $1s$ AO of the bridging hydrogen atom (27%) and by the $4p_x$ AO of the metal atoms (25%).

Thus H_B1s AO participates in the formation of only three bonding molecular levels, viz. $13a_1$, $14a_1$ and $15a_1$ whose energies differ only slightly from those of the respective molecular levels in the triple carbonyl bridged dimer shown in Figs. 3,5. We emphasize here that the energy difference between the last filled molecular level of the Fe–H–Fe bridge bond character and the HOMO level is relatively large (6.66 eV), which indicates fairly high stability of the Fe–H–Fe bridge bond in that complex.

The higher filled molecular levels corresponding to the $d\mathrm{Fe}\rightarrow\Pi^a\mathrm{CO_T}$ or $d\mathrm{Fe}\rightarrow\Pi^a\mathrm{CO_B}$ interactions in

$(CO)_3Fe\langle^{CO}_{CO}\rangle Fe(CO)_3$

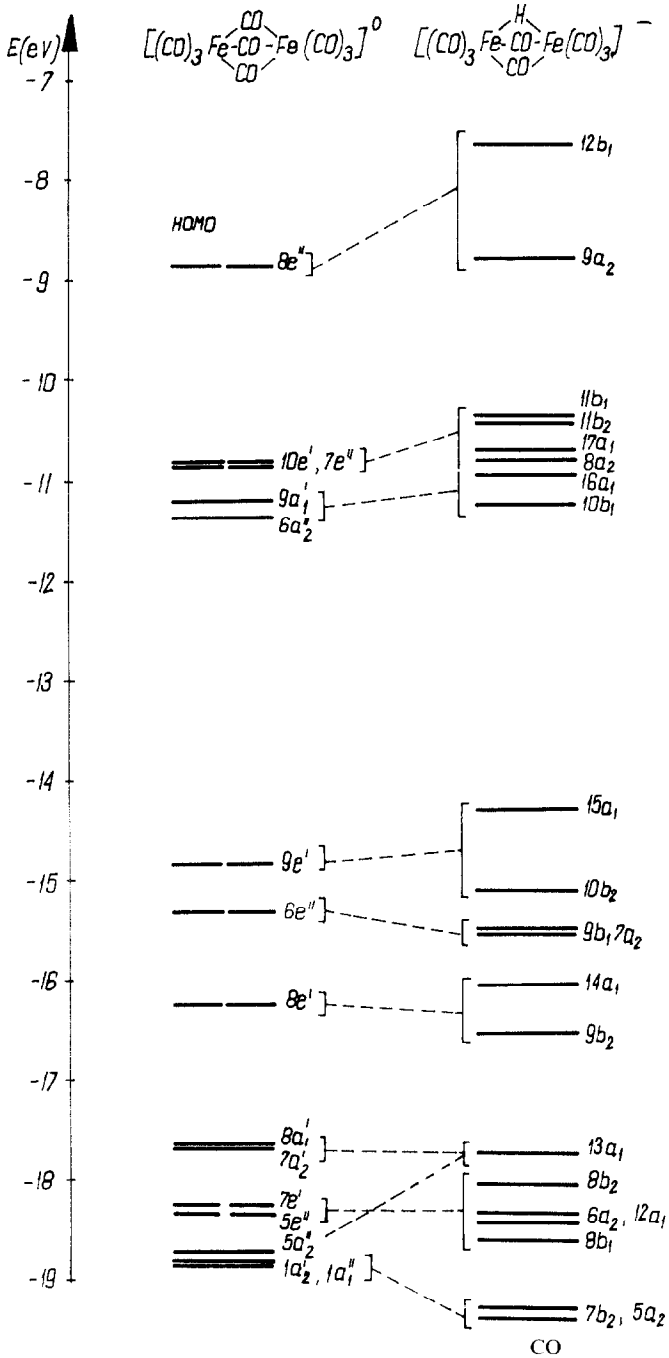

Fig. 3. Correlation of the molecular levels of $(CO)_3Fe\langle^{CO}_{CO}\rangle Fe(CO)_3$ and $[(CO)_3Fe\langle^{H}_{CO}\rangle Fe(CO)_3]^-$.

change neither in their energy nor composition. Only the degenerated levels, viz. $10e'$ and $7e''$ undergo slight splitting. On the other hand, splitting of the HOMO ($8e''$) level is quite considerable.

Table 3

Energies and compositions of highest occupied molecular levels of $[(CO)_3Fe\langle^{H}_{CO}\rangle Fe(CO)_3]^-$, with C_{2v} symmetry

MO	Energy (eV)	Largest contributions of the valence atomic orbitals (%)					
$18a_1$ LUMO	−5.74	$3d_{z^2}$(Fe)	30	p_y(O)	25	p_y(C)	19
$12b_1$ HOMO	−7.66	$3d_{xz}$(Fe)	48	p_x(Fe)	19	$p_y(O_B)$	7
$9a_2$	−8.76	$3d_{yz}$(Fe)	40	p_y(Fe)	18	p_y(C)	15
$11b_1$	−10.38	$3d_{x^2-y^2}$(Fe)	76	p_x(O)	7	p_y(O)	4
$11b_2$	−10.46	$3d_{xy}$(Fe)	75	$3d_{yz}$(Fe)	6	$p_x(O_B)$	3
$17a_1$	−10.74	$3d_{x^2-y^2}$(Fe)	70	$p_x(O_B)$	9	$3d_{xz}$(Fe)	5
$8a_2$	−10.79	$3d_{xy}$(Fe)	68	$p_y(O_B)$	15	$p_x(O_B)$	4
$16a_1$	−10.97	$3d_{z^2}$(Fe)	58	p_x(O)	12	s(Fe)	9
$10b_1$	−11.24	$3d_{z^2}$(Fe)	28	$p_y(O_B)$	22	s(Fe)	17
$15a_1$	−14.32	$s(H_B)$	27	p_x(Fe)	25	p_x(O)	15
$10b_2$	−15.13	p_x(O)	27	p_y(O)	19	p_y(Fe)	17
$7a_2$	−15.52	p_y(O)	35	$3d_{xz}$(Fe)	18	p_x(O)	12
$9b_1$	−15.53	p_x(O)	25	p_y(O)	24	$3d_{xz}$(Fe)	18
$14a_1$	−16.03	$3d_{xz}$(Fe)	36	$s(H_B)$	17	p_x(O)	14
$9b_2$	−16.56	$p_z(O_B)$	28	$3d_{yz}$(Fe)	25	$p_z(C_B)$	17
$13a_1$	−17.79	$p_x(O_B)$	45	$p_z(C_B)$	21	p_z(Fe)	9
$8b_2$	−18.07	$p_x(O_B)$	64	$p_x(C_B)$	32	$p_z(O_B)$	2
$12a_1$	−18.37	$p_x(O_B)$	57	$p_x(C_B)$	37	$p_z(O_B)$	3
$6a_2$	−18.43	$p_y(O_B)$	51	$p_y(C_B)$	36	$3d_{yz}$(Fe)	3
$8b_1$	−18.59	$p_y(O_B)$	53	$p_y(C_B)$	40	s(Fe)	3
$5a_2$	−19.26	p_x(O)	87	p_x(C)	13		
$7b_2$	−19.37	p_x(O)	87	p_x(C)	13		

Since no essential changes occur in the contribution of the atomic orbitals of iron to the formation of the molecular levels, the Fe–Fe interaction in the

$[(CO)_3Fe\langle^{H}_{CO}\rangle Fe(CO)_3]^-$

complex reveals an antibonding character. The value of the Fe–Fe overlap population equal to −0.170 is almost the same as that of the complex with a triple carbonyl bridge. Thus, on going from the bridge core

$Fe\langle^{CO}_{CO}\rangle Fe$ to $Fe\langle^{H}_{CO}\rangle Fe$,

because of the antibonding character of the Fe–Fe interaction, a decrease in the distance between the metal atoms is not favourable (Table 4). A shorter distance between the metal atoms would result in increased overlap between the $3d_{xz}$, $3d_{yz}$, $4p_x$, $4p_y$ AOs of the Fe atoms, and so in an increase of the negative value of the Fe–Fe overlap population, that is, in an increase in the antibonding Fe–Fe interaction.

The results of the population analysis are also indicative of certain similarities in the character of the Fe–H–Fe and Fe–CO–Fe bonds in the

$[(CO)_3Fe\langle^{H}_{CO}\rangle Fe(CO)_3]^-$

complex. A small negative charge on the H atom of -0.080 corresponds to a small negative charge on the bridge CO_B group of -0.141 (Table 4).

In the complex with a triple carbonyl bridge a charge of -0.031 is localized on the CO_B groups. Thus, the insertion of the hydrogen bridge results in a slight increase of the electron density on all bridging ligands.

Furthermore the overlap population of the $3d$ orbitals in the iron atoms with the atomic orbitals of carbon of the CO_B groups in

$$[(CO)_3Fe\langle \overset{H}{\underset{CO}{CO}} \rangle Fe(CO)_3]^-$$

(dFe–C_B) being equal to 0.095, is in the same order as the overlap population of the $3d$ orbitals of the Fe atoms with the $1s$ orbital of the hydrogen atom (dFe–$1sH_B$), which is equal to 0.059.

Owing to the fact that a negative charge is localized on iron atoms, the bridge bonds Fe–H–Fe and Fe–CO–Fe in the complex

$$[(CO)_3Fe\langle \overset{H}{\underset{CO}{CO}} \rangle Fe(CO)_3]^-$$

have covalent character only. It is also interesting that on replacing one of the CO_B groups in the

$$(CO)_3Fe\langle \overset{CO}{\underset{CO}{CO}} \rangle Fe(CO)_3$$

complex with a hydrogen atom, practically no changes occur in the charges localized on the metal atoms. On the other hand, significant changes occur in charges localized both on the CO_B and CO_T groups. As mentioned above, the negative charge on the bridging carbonyl groups increases, whereas the positive charge on the terminal carbonyl groups decreases (Table 4). This indicates that the dFe$\rightarrow\Pi^a CO_B$ and dFe$\rightarrow\Pi^a CO_T$ interactions are stronger in

$$[(CO)_3Fe\langle \overset{H}{\underset{CO}{CO}} \rangle Fe(CO)_3]^-$$

than in

$$(CO)_3Fe\langle \overset{CO}{\underset{CO}{CO}} \rangle Fe(CO)_3.$$

For the terminal ligands these interactions are slightly weaker for the carbonyl groups in positions *trans* to the bridging hydrogen atom (CO_T^t) than for the carbonyl groups in *cis* position to the bridging hydrogen atom (CO_T^c) since the charges on (CO_T^t) and (CO_T^c) are not equal, being $+0.096$ and $+0.054$, respectively.

The overlap population for Fe–CO_T^t, of $+0.186$, is slightly lower than that for Fe–C_T^c of $+0.202$. Thus, the covalent Fe–CO_T^t bond is slightly weaker than the covalent Fe–CO_T^c bond. On the other hand because of the negative charges on the metal atoms and higher positive charges on (CO_T^t) than on (CO_T^c), a stronger ionic Fe–CO_B^t bond compared with the ionic Fe–CO_T^c bond results.

Table 4

Mulliken atomic charges and overlap populations [a]

Compound	$(CO)_3Fe\langle^{CO}_{CO}\rangle Fe(CO)_3$	$[(CO)_3Fe\langle^{H}_{CO}\rangle Fe(CO)_3]^-$	$[Cl_3Mo\langle^{Cl}_{Cl}\rangle MoCl_3]^{3-}$	$[Cl_3Mo\langle^{H}_{Cl}\rangle MoCl_3]^{3-}$
Atomic charges				
M	−0.505	−0.522	1.043	1.114
L_B	−0.031	−0.141	−0.560	−0.475
H_B	–	−0.080	–	−0.534
L_T	0.184	0.054(*c*)	−0.568	−0.619(*c*)
		0.096(*t*)		−0.626(*t*)
Overlap populations				
M–M	−0.166	−0.170	0.142	0.336
dM–L_B	0.092	0.095	0.052	0.066
s,pM–L_B	0.166	0.178		
M–L_B	0.258	0.273	0.094	0.133
dM–H_B	–	0.059	–	0.084
s,pM–H_B	–	0.114	–	0.032
M–H_B	–	0.173	–	0.133
d_M–L_T	0.125	0.120(*c*)	0.088	0.098(*c*)
		0.140(*t*)		0.100(*t*)
s,pM–L_T	0.066	0.082(*c*)	0.062	0.086(*c*)
		0.046(*t*)		0.074(*t*)
M–L_T	0.191	0.202(*c*)	0.150	0.184(*c*)
		0.186(*t*)		0.174(*t*)

[a] B = bridge ligand, T = terminal ligand, *c* = *cis* to bridge hydrogen atom, *t* = *trans* to bridge hydrogen atom.

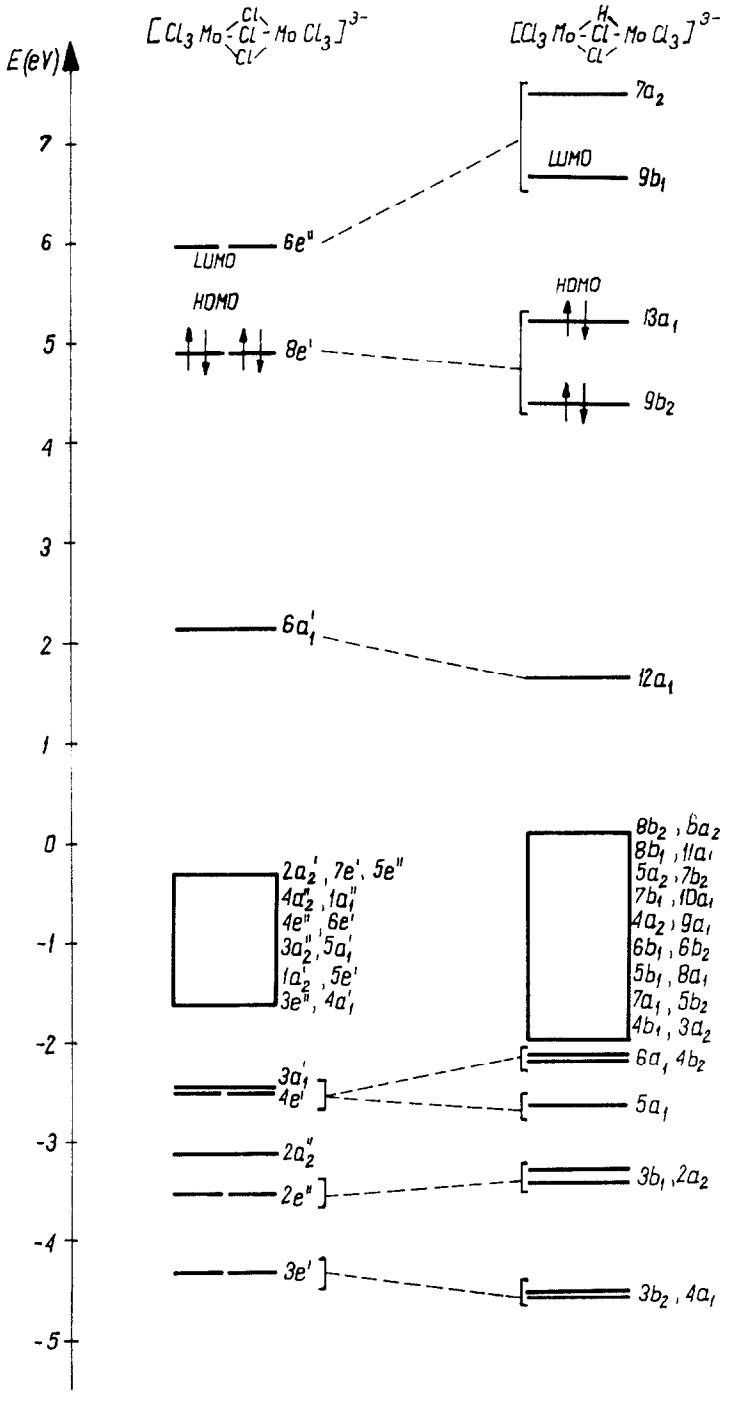

Fig. 4. Correlation of the molecular levels of $[Cl_3Mo(\mu\text{-}Cl)_3MoCl_3]^{3-}$ and $[Cl_3Mo(\mu\text{-}H)(\mu\text{-}Cl)_2MoCl_3]^{3-}$.

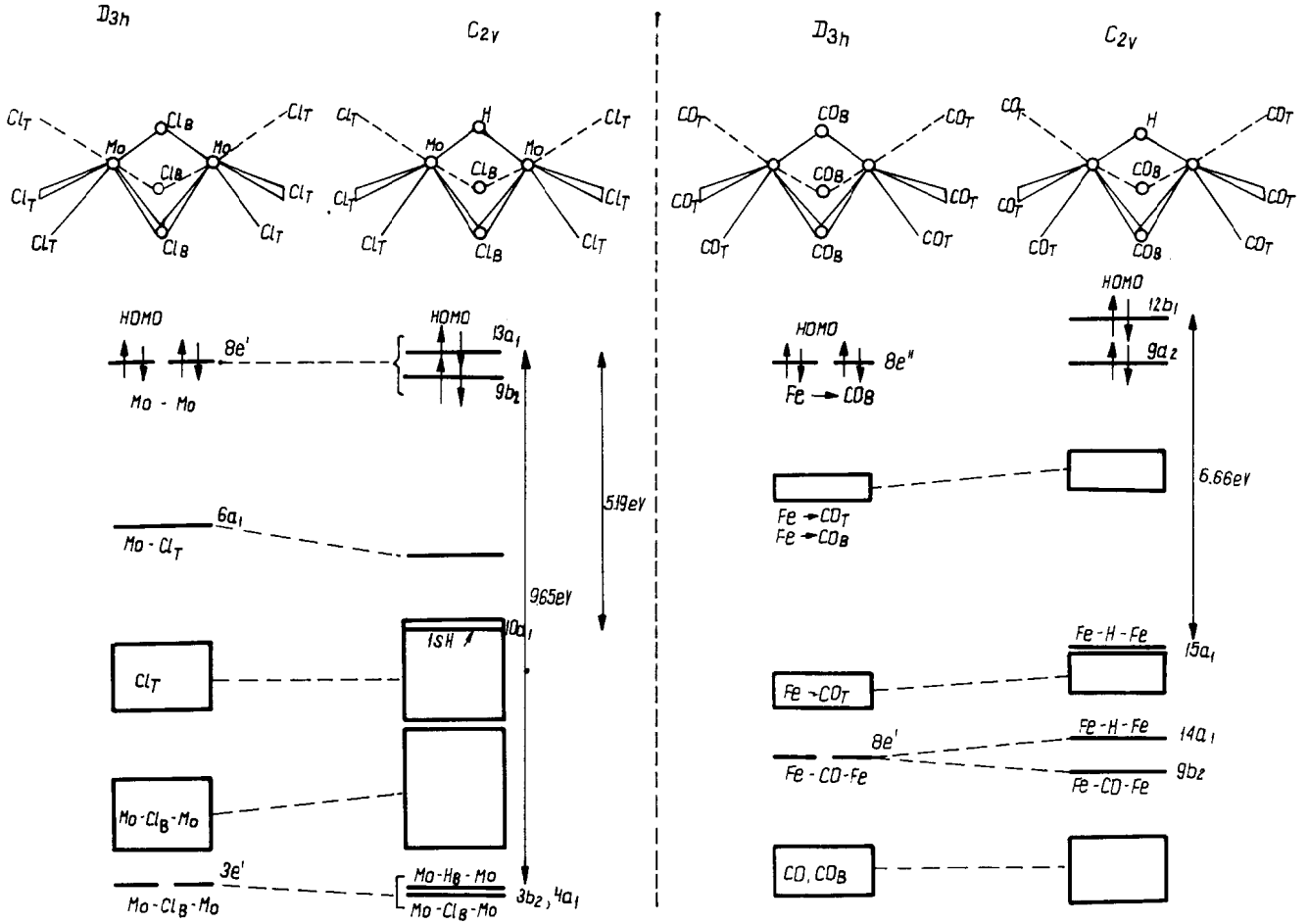

Fig. 5. Comparison of the role of the hydrogen atom in the formation of triple mixed bridges in $[Cl_3Mo\overset{H}{\underset{Cl}{<}}Cl>Mo\ Cl_3]^{3-}$ and $[(CO)_3Fe\overset{H}{\underset{CO}{<}}CO>Fe(CO)_3]^{-}$.

So in contrast to covalent bonding effects, the ionic bonding effects should shorten the Fe–CO_T^t bond with respect to Fe–CO_T^c bond and this results in the experimentally stated equal distances for Fe–CO_T^c and Fe–CO_T^t, which may also be described in terms of comparable *trans* effects of bridging carbonyl group and bridging hydrogen atom. In our calculations we have also allowed for the fact that the Fe–CO_B bonds are about 0.2 A longer than the Fe–CO_T bonds. In spite of this, $d\mathrm{Fe}\rightarrow\Pi^a\mathrm{CO}_B$ interaction is stronger than $d\mathrm{Fe}\rightarrow\Pi^a\mathrm{CO}_T$ interaction, as evidenced by the negative charges on the CO_B groups. Also the overlap population of Fe–CO_B (+0.258) is higher than that of Fe–CO_T (+0.191). Thus the covalent bonds Fe–CO_B are stronger than the covalent Fe–CO_T bonds. So the elongation of Fe–CO_B bonds with respect to the Fe–CO_T bonds most probably is due to the lack of ionic effects in the Fe–CO_B bonds because of the negative charges localized on the iron atoms and CO_B groups.

2. Comparison of the Mo–H–Mo and Mo–Cl–Mo bridge bonds in the $[Cl_3Mo(\mu\text{-}Cl)_3MoCl_3]^{3-}$ *and* $[Cl_3Mo(\mu\text{-}H)(\mu\text{-}Cl)_2MoCl_3]^{3-}$ *complexes*

The sequence of filled energy levels, formed from the valence $3s$ and $3p$ atomic orbitals of chlorine and the $4d,5s,5p$ and $5d$ atomic orbitals of molybdenum and determined by use of the Fenske–Hall method by Natkaniec [9] for

$[Cl_3Mo(\mu\text{-}Cl)_3MoCl_3]^{3-}$

may be generally described as follows, in increasing energy:

(*1*) non-bonding levels of the $3s$ type AOs of the bridging chlorine atoms (Cl_B) or terminal chlorine atoms (Cl_T)

(*2*) levels of the Mo–Cl–Mo bridge bonds in which the main contribution is provided by the $2p_x$, $2p_y$, $2p_z$ atomic orbitals of the bridge ligands Cl_B (30–70%) and the $4d_{xz}$, $4d_{yz}$, $4d_{xy}$, $4d_{x^2-y^2}$, $4d_{z^2}$, $5s$ atomic orbitals of the metal atoms (10–20%)

(*3*) non-bonding molecular levels mainly of the $3p$ AOs of the Cl_B and Cl_T ligands

(*4*) the $6a_1$ level corresponding mainly to the Mo–Cl_T bonds and Mo–Mo bonding interactions of the σ type

(*5*) the $8e'$ level corresponding mainly to Mo–Mo bonding interactions of the Π and δ type

Thus there is a direct metal–metal bond in this complex and this is reflected in the positive value of the two-centre overlap population of Mo–Mo, viz. 0.142.

A correlation of the last filled levels in the complexes:

$[Cl_3Mo(\mu\text{-}Cl)_3MoCl_3]^{3-}$

with D_{3h} symmetry and

$[Cl_3Mo(\mu\text{-}H)(\mu\text{-}Cl)_2MoCl_3]^{3-}$

with C_{2v} symmetry is shown in Figs. 4, 5.

Table 5

Energies and compositions of the highest occupied molecular levels of $[Cl_3Mo\overset{H}{\underset{Cl}{<Cl>}}MoCl_3]^{3-}$ with C_{2v} symmetry

MO	Energy (eV)	Largest contribution of the valence atomic orbitals (%)					
$9b_1$ LUMO	6.66	$4d_{x^2-y^2}$(Mo)	62	$4d_{xz}$(Mo)	12	$4d_{z^2}$(Mo)	10
$13a_1$ HOMO	5.18	$4d_{x^2-y^2}$(Mo)	50	$4d_{xz}$(Mo)	28	$p_x(Cl_B)$	9
$9b_2$	4.40	$4d_{xy}$(Mo)	46	$4d_{yz}$(Mo)	33	p_x(Cl)	12
$12a_1$	1.67	$4d_{z^2}$(Mo)	47	p_y(Cl)	36	p_z(Cl)	9
$6a_2$	0.08	p_x(Cl)	39	p_y(Cl)	38	p_z(Cl)	22
$8b_2$	0.07	p_x(Cl)	43	p_y(Cl)	38	p_z(Cl)	18
$11a_1$	0.04	p_x(Cl)	48	p_x(Cl)	26	p_z(Cl)	26
$8b_1$	0.04	p_y(Cl)	47	p_x(Cl)	30	p_z(Cl)	23
$7b_2$	0.03	p_x(Cl)	80	p_y(Cl)	13	p_z(Cl)	7
$5a_2$	0.02	p_x(Cl)	92	p_y(Cl)	5	p_z(Cl)	2
$10a_1$	−0.01	$s(H_B)$	41	p_z(Cl)	37	p_y(Cl)	11
$7b_1$	−0.25	p_y(Cl)	64	$p_y(Cl_B)$	12	p_z(Cl)	12
$9a_1$	−0.32	p_x(Cl)	56	$p_x(Cl_B)$	20	p_y(Cl)	18
$4a_2$	−0.44	p_x(Cl)	56	p_y(Cl)	27	$p_y(Cl_B)$	9
$6b_2$	−0.58	p_x(Cl)	56	$p_y(Cl_B)$	19	$4d_{xy}$(Mo)	5
$6b_1$	−0.59	p_z(Cl)	57	p_x(Cl)	37	p_y(Cl)	6
$8a_1$	−0.62	p_z(Cl)	59	p_y(Cl)	15	$p_z(Cl_B)$	8
$5b_1$	−0.76	p_x(Cl)	36	p_z(Cl)	32	p_y(Cl)	16
$5b_2$	−0.93	p_z(Cl)	43	$p_z(Cl_B)$	25	p_y(Cl)	22
$7a_1$	−1.37	p_y(Cl)	45	$4d_{z^2}$(Mo)	32	$p_z(Cl_B)$	13
$3a_2$	−1.49	p_z(Cl)	46	$p_y(Cl_B)$	22	p_y(Cl)	12
$4b_1$	−1.99	p_z(Cl)	47	p_y(Cl)	27	$4d_{xz}$(Mo)	9
$4b_2$	−2.01	$p_x(Cl_B)$	76	p_x(Cl)	8	$4d_{xy}$(Mo)	8
$6a_1$	−2.05	$p_z(Cl_B)$	38	p_z(Cl)	15	$4d_{z^2}$(Mo)	15
$5a_1$	−2.63	$p_x(Cl_B)$	73	$4d_{x^2-y^2}$(Mo)	13	p_x(Cl)	8
$2a_2$	−3.28	$p_y(Cl_B)$	56	$4d_{xy}$(Mo)	17	p_z(Cl)	12
$3b_1$	−3.38	$p_y(Cl_B)$	66	p_y(Cl	10	$4d_{z^2}$(Mo)	8
$4a_1$	−4.47	$4d_{xz}$(Mo)	29	$p_z(Cl_B)$	26	$s(H_B)$	19

When one of the chlorine bridges is replaced with a hydrogen bridge, after transition to the

$$[Cl_3Mo\overset{H}{\underset{Cl}{<Cl>}}MoCl_3]^{3-}$$

complex, significant changes in the energy values and compositions of the energy levels are observed mainly in the group of the bridge levels, which is similar to that for case of the iron carbonyls discussed above (Table 5). These changes consist in replacing the $3e'$ level formed mainly by the $2p_z$ AOs of the Cl_B atoms and $4d_{xz}$ and $4d_{yz}$ AOs of the Mo atoms with the two levels: $3b_2$ and $4a_1$.

The $3b_2$ orbital still corresponds to the Mo–Cl–Mo bridge bond whereas $4a_1$ now also contains the contribution by the $1s$ H_B AO (19%) which corresponds to both the Mo–Cl–Mo and Mo–H–Mo bonds. The higher group of energy levels has non-bonding character, which consist exclusively of the $3p$ AOs of the Cl_T atoms. The contributions derived from the $3p$ orbitals of the Cl_B atoms were replaced by the $1s$ AO contribution by the bridging hydrogen atom also in the $10a_1$ energy level.

The $10a_1$ level, which owing to a very low contribution by the atomic metal d orbitals (4%), should also be considered to be a M–H–M bridge level. One may note that analogous with this level ($10a_1$), the $15a_1$ energy level in

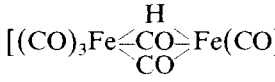

undoubtedly corresponds to the M–H–M bridge bond, owing to a fairly high contribution by the metal orbitals in it. In this case it is a contribution by both *d* and *p* metal orbitals.

The fact that all molecular orbitals corresponding to the bridge bonds Mo–Cl–Mo and Mo–H–Mo in

are situated in the energy range corresponding to the bridge bonds in

might indicate comparable stabilities of the triple bridges in these two complexes analogous to the iron carbonyls

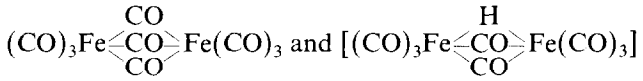

discussed above. Replacement of one of the bridge chlorine atoms with the hydrogen atom thus going from

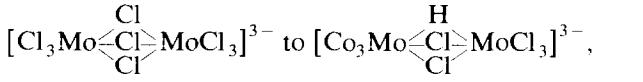

only slightly influences those levels with high contributions from the atomic metal orbitals which also resemble the above-mentioned iron carbonyls. Owing to a decrease in symmetry, the degeneration of the HOMO, $8e'$, level is removed but the quantitative and qualitative composition of $9b_2$ and $13a_1$ levels is analogous to that of the $8e'$ level, implying there is also a direct bond between the metal atom in the

complex.

Because of the decrease in the metal–metal distance on transition to the hydrogen bridge complex, studied for the calculations, the positive value of two-centre overlap population of Mo–Mo increased from +0.142 in

to +0.336 in

Thus, in the case of the molybdenum chloride dimers, contrary to iron carbonyl dimers, a decrease in the interatomic distance is favourable since it increases the covalent strength of M–M bond. The slight change in the distribution of charges on the metal atoms and bridge ligands when one Cl atom is replaced with one H atom in the

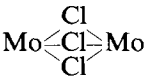

bridge core is also characteristic.

The negative charges on the bridge chlorine atoms decrease from -0.560 to -0.475 with a simultaneous increase in the positive charges on the metal atoms from $+1.043$ up to $+1.114$. By contrast, the negative charge on the bridge hydrogen atom of -0.534 is close to that on the bridge chlorine in the complex with a triple chlorine bridge.

Thus, in a mixed bridge the electron density is somewhat shifted towards the hydrogen atom. In other words, the Mo–H–Mo bond has a slightly stronger ionic character than the Mo–Cl–Mo bond.

The overlap populations of Mo–H and Mo–Cl_B differ only slightly and are 0.116 and 0.133 respectively. This is indicative of the comparable covalent natures of the Mo–H–Mo and Mo–Cl–Mo bonds.

It deserves mention that also in the other two complexes investigated by us by use of the Fenske–Hall method viz.

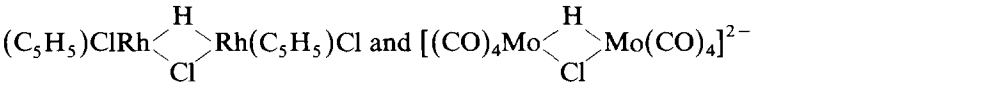

in which the metal atoms are bridged simultaneously by hydrogen and chlorinate aotm, the M–H–M bond has slightly stronger ionic character than M–Cl–M bond [10].

The covalent nature of the M–H–M and M–Cl–M bonds in these complexes is also comparable.

Under the same Mo–Cl_T^c and Mo–Cl_T^t bond lengths assumed in the calculations for

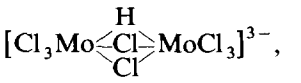

a somewhat lower overlap population Mo–Cl_T^t compared with Mo–Cl_T^c shows that the bond of the metal atom with the terminal ligands *trans* to the bridging hydrogen is weaker than those which are *cis*. This may result in elongation of the Mo–Cl_T^t bond in respect to Mo–Cl_T^c bond. Thus we can say that the *trans* effect of the bridge hydrogen atom is a little stronger than the *trans* effect of the bridge chlorine atom.

Conclusions

We have stated that on going from

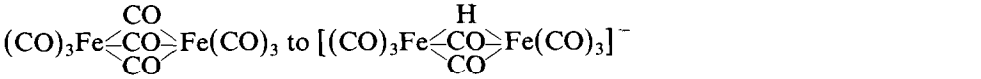

and from

$$[Cl_3Mo\overset{Cl}{\underset{Cl}{<}}Cl>MoCl_3]^{3-} \text{ to } [Cl_3Mo\overset{H}{\underset{Cl}{<}}Cl>MoCl_3]^{3-}$$

the molecular levels corresponding to the M–H–M bridged bond are located in the same energy as the molecular levels, corresponding to the M–L–M bond, replacing it (Fig. 5).

After one of the bridge ligand is replaced by the hydrogen atom, the electron density distribution for bridge cores remains almost unchanged. The M–H–M bond exhibits the same character as the M–L–M bonds, because the negative charge on the hydrogen atom is almost equal to that on ligand L, and the M–H overlap population does not deviate too much from M–L overlap population. Thus, the Mo–H–Mo bond in

$$[Cl_3Mo\overset{H}{\underset{Cl}{<}}Cl>MoCl_3]^{3-}$$

complex shows the partial ionic character of the carbonyl complexes with single and double bridges

$$[(CO)_5Mo\text{–}H\text{–}Mo(CO)_5]^- \text{ and } [(CO)_4Mo\overset{H}{\underset{H}{<}}>Mo(CO)_4]^{2-}.$$

By contrast, the Fe–H–Fe bond in

$$[(CO)_3Fe\overset{H}{\underset{CO}{<}}CO>Fe(CO)_3]^-$$

is exclusively covalent like that of the single hydrogen bridge in the carbonyl complex $[(CO)_4Fe\text{–}H\text{–}Fe(CO)_4]^-$ [2]. It should be emphasized again, that the character of the M–H–M bond depends on the nature of the metal atom. In the complex

$$[Cl_3Mo\overset{H}{\underset{Cl}{<}}Cl>MoCl_3]^{3-}$$

there is a strong direct Mo–Mo bonding and in the complex there is

$$[(CO)_3Fe\overset{H}{\underset{CO}{<}}CO>Fe(CO)_3]^-$$

strong Fe–Fe antibonding interaction, which is virtually absent from the previously discussed carbonyl dimers with single and double hydrogen bridges [2]. From our calculations it is clear that the *trans* effect of the bridging hydrogen atom is comparable with that of the bridging carbonyl group and is somewhat stronger than that of the bridging chlorine atom.

Acknowledgement

This work was supported financially by the Project No. CPBP 01.12 of Polish Academy of Sciences.

References

1 (a) J.L. Petersen and J.M. Williams, Inorg. Chem., 17 (1978) 1308; (b) N.J. Cooper, M.L.H. Green, C. Couldwell, K. Prout, J. Chem. Soc., Chem. Commun., (1978) 145; (c) R.J. Doedens, W.T. Robinson, J.A. Ibers, J. Am. Chem. Soc., 89 (1967) 4323; (d) M.R. Churchill and S.W.Y. Ni, J. Am. Chem. Soc., 95 (1973) 2150.
2 B. Jeżowska-Trzebiatowska and B. Nissen-Sobocińska, J. Organomet. Chem., 322 (1987) 331.
3 H.B. Chin and R. Bau, Inorg. Chem., 17 (1978) 2314.
4 A. Bino and F.A. Cotton, Angew. Chem., 91 (1979) 356.
5 F.A. Cotton and J.M. Troup, J. Chem. Soc., Dalton Trans., (1974) 800.
6 A. Bino and F.A. Cotton, J. Am. Chem. Soc., 101 (1979) 4150.
7 M.B. Hall and R.F. Fenske, Inorg. Chem., 11 (1972) 768.
8 A.P. Ginsberg, J. Am. Chem. Soc., 102 (1982) 111.
9 L. Natkaniec, Bull. Acad. Polon Sci., Ser. Sci. Chim., 26 (1978) 633.
10 A. Bino, B.E. Burnsten, F.A. Cotton and A. Fang, Inorg. Chem., 21 (1982) 3755.
11 B. Jezowska-Trzebiatowska and B. Nissen-Sobacińska, J. Organomet. Chem., 342 (1988) 215.